ELSEVIER

Coordination Chemistry Reviews
197 (2000) 249–276

COORDINATION CHEMISTRY REVIEWS

www.elsevier.com/locate/ccr

Chemical bonding in mononuclear transition metal complexes with Group 13 diyl ligands ER (E = B–Tl) Part X: Theoretical studies of inorganic compounds☆

Christian Boehme [1], Jamal Uddin, Gernot Frenking *

Fachbereich Chemie, Philipps-Universität Marburg, Hans-Meerwein-Strasse, D-35037 Marburg, Germany

Received 2 June 1999; accepted 27 August 1999

This paper is dedicated to Professor Ronald J. Gillespie on the occasion of his 75th birthday.

Contents

☆ Part IX: A. Beste, O. Krämer, A. Gerhard, G. Frenking, Eur. J. Inorg. Chem. (1999) 2037.

* Corresponding author. Fax: +49-6421-282-8917.
E-mail address: frenking@chemie.uni-marburg.de (G. Frenking)
[1] Present address: Université Luis Pasteur, Strasbourg, France.

PII: S0010-8545(99)00227-1

Abstract

Recent advances in the synthesis of stable transition metal complexes with terminal BR, AlR, GaR and InR ligands where R is mostly but not always a π-donor ligand, gave rise to speculation about metal–ligand binding interactions. In response to this, theoretical studies have been carried out, which focus on the nature of the chemical bond in transition metal complexes with terminal Group 13 diyl ligands ER (E = B–Tl). Some of these investigations were made in cooperation with experimental work which reported new stable complexes. The theoretical work made predictions about the geometries and bond energies of the complexes. The bonding situation of the TM–ER bonds, which has been controversial in the literature, has also been examined. The review summarizes the results and the progress in the understanding of the nature of the TM–ER bonds which has been gained in recent theoretical work. Previous discussions focused on the importance of RE → TM σ donation and particularly the RE ← TM π-backdonation. The analysis of the bonding situations revealed that the π-backdonation may indeed become as important as RE → TM σ donation, but the total covalent TM–ER bond order is always less than 1. The most important conclusion which arises from these theoretical studies is that the TM–ER bonding interactions are largely ionic, and that the covalent donor–acceptor interactions play a less important role. This makes the discussion whether the TM–ER bond should be considered as a single or triple bond irrelevant.

Keywords: Chemical bonding; Mononuclear transition metal complexes; Diyl ligands

1. Introduction

The chemistry of transition metal (TM) complexes with ligand atoms of Group 13 has made remarkable progress in the last few years. Highlights of the development are the spectacular syntheses of the stable mononuclear species $L_nTM–ER$ where the Group 13 ligand atom is in the +1 formal oxidation state [1]. Prominent examples are $(CO)_4Fe–AlCp^*$ [2], the first terminal borylene complexes $(CO)_4Fe–BCp^*$ [3] and $(CO)_4W–BN(SiMe_3)_2$ [4], the 'ferrogallyne' $(CO)_4Fe–GaAr^*$ ($Ar^* = 2,6$-(2,4,6-triisopropylphenyl)-phenyl) [5], and the homoleptic complexes $Ni(E–C(SiMe_3)_3)_4$ with E = In [6] and E = Ga [7]. It has long been speculated that TM complexes with the ligand BF, which is isoelectronic to CO, might become isolable under appropriate conditions [8]. Recent theoretical studies of the bonding properties of TM–BF complexes led to the conclusion that BF should, in principle, be an excellent ligand and be a better σ donor and comparable π acceptor than CO, but the high polarity of BF and the buildup of positive charge should lead to a low kinetic stability [9–11]. Larger R substituents that provide steric protection in complexes $L_nTM–BR$ might accomplish the goal of isolable terminal borylene complexes, but electronic factors should be very important for the stability of the compounds [9]. Most discussions about the binding interactions in TM–ER complexes focused on three factors: (a) ER ← TM π-backdonation, (b) TM–E ← R π-donation, and (c) steric shielding of the R group. A better knowledge of the contribution of each factor to the stabilization of diyl complexes would be very helpful in the synthesis of new complexes.

The importance of the three factors (a–c) have been discussed. In particular, the Ga ← Fe π-backdonation in $(CO)_4$Fe–GaAr* was the topic of heated discussion [12]. While Robinson interpreted the short Fe–Ga bond in the dicoordinated Ga compound with linear Fe–Ga–C(Ar) arrangement as a triple bond [5], Cotton dismissed the idea of strong Ga ← Fe π-backdonation and suggested a Fe–Ga single bond [13]. Recent theoretical studies showed that the Ga ← Fe π-backdonation in $(CO)_4$Fe–GaPh is indeed stronger than in gallanediyl complexes L_nTM–GaR where R is a π-donor-substituent [14,16]. However, an important result of these studies was the observation that the Fe–Ga bonding in $(CO)_4$Fe–GaPh is largely ionic in nature, and that the donor–acceptor interactions give a covalent bond order of less than 1, which makes the discussion about a single or triple bond between Fe and Ga meaningless. It seems that too much emphasis has been placed on donor–acceptor interactions in TM–ER bonding, while the dominant contributions of the charge interactions to the metal–ligand binding in Group 13 diyl complexes have perhaps been underestimated.

Fig. 1 shows the principle orbital interactions in TM complexes with Group 13 ligands ER. Much insight into the nature of the TM–ER bond with different groups R has been gained by recent theoretical studies of our group [2,7,14–17] and by others [9–11,13] who analyzed the binding interactions using different methods for the population and energy analysis. This review summarizes the most important results of recent theoretical work which make it possible to understand the nature of the chemical bonding in TM complexes with terminal ER ligands. The bonding picture which emerges from this work should also be helpful in the design of future experiments.

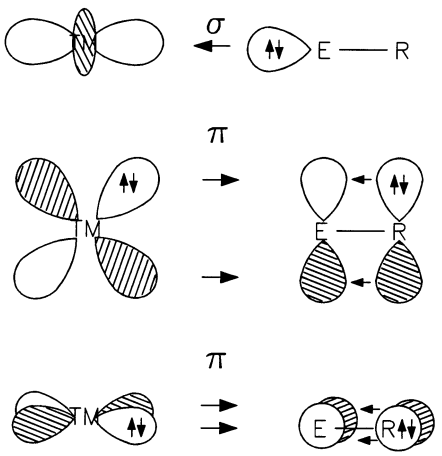

Fig. 1. Principle donor–acceptor interactions in transition metal Group 13 diyl complexes L_nTM–ER where R carries the π lone-pair electrons.

2. Theoretical methods

The theoretical work about the nature of the TM–ER bond published so far used either standard ab initio calculations or gradient corrected DFT methods. Systematic theoretical studies have shown that the geometries and bond energies of electronically saturated TM complexes can be calculated with high accuracy using relativistic effective core potentials (ECPs) which retain the outer-core electrons of the TMs [18] in conjunction with a DZP valence basis set [19]. The details of these methods can be found in the original papers. Some of the methods for analyzing the bonding situations that were used are less common and thus, shall briefly be introduced.

One method is the energy partitioning scheme ETS (extended transition state), which was developed by Ziegler and Rauk [20]. The basic ideas, which are the same as earlier ones introduced by Morokuma [21], are the following [22]. The overall bond energy ΔE of a bond A–B is broken down into four components which are calculated separately in four consecutive steps:

$$\Delta E = \Delta E_{\text{prep}} + \Delta E_{\text{elst}} + \Delta E_{\text{Pauli}} + \Delta E_{\text{orb}} \quad (1)$$

In the present case we are interested in the L_nTM–ER bonds. ΔE_{prep} is then the energy difference between the fragments L_nTM and ER in their equilibrium geometry and electronic ground state and in the geometry and electronic state which they acquire in the complex L_nTM–ER. ΔE_{elst} is the electrostatic interaction energy between the fragments which are calculated with a frozen electron density distribution in the geometry of the complex. This term is usually attractive. ΔE_{Pauli} gives the repulsive energy caused by exchange (Pauli) repulsion, which is calculated when the wavefunction after step two becomes orthogonalized and antisymmetrized. The energy terms ΔE_{elst} and ΔE_{Pauli} are frequently summed up to give the so-called steric term $\Delta E°$, which should not be confused with the loosely defined steric interaction between substituents in a molecule. The final term ΔE_{orb} gives the stabilization which comes from the orbital interactions when the wavefunction in step four is relaxed. The latter term can be broken down into orbital contributions with different symmetry. This makes it possible to calculate energy contributions due to σ and π interactions.

The CDA (charge decomposition analysis) [23] was developed as a quantitative expression of the Dewar–Chatt–Duncanson (DCD) model [24] of synergic metal–ligand bonding, which considers the ligand $\rightarrow$ metal σ-donation and ligand $\leftarrow$ metal π-backdonation as the dominant factors for the metal–ligand bond. In the CDA, the wavefunction of the complex L_nTM–X is expressed as a linear combination of the fragment molecular orbitals of the ligand X (in the present case ER) and the remaining metal fragment L_nTM. The orbital contributions are divided into four parts: (i) mixing of the occupied σ-type MOs of ER and the unoccupied σ-type MOs of L_nTM (σ-donation RE $\rightarrow$ TML_n); (ii) mixing of the unoccupied π-type MOs of ER and the occupied π-type MOs of L_nTM (π-backdonation RE $\leftarrow$ TML_n); (iii) mixing of the occupied MOs of ER and the occupied MOs of L_nTM (repulsive polarization RE $\leftrightarrow$ TML_n); (iv) mixing of the unoccupied MOs of ER and the

unoccupied MOs of L_nTM (rest term Δ). The latter term should not contribute to the electronic structure of the complex. It has been found that the rest term is a sensitive probe if the compound can be classified as a donor–acceptor complex. A significant deviation from $\Delta = 0$ indicates that the bond L_nTM–ER has the character of a normal covalent bond between two open-shell fragments, rather than a donor–acceptor bond between a Lewis acid and a Lewis base [25].

3. TM complexes with ligands ER

In the following sections we will summarize the results of recent theoretical studies that address the chemical bonding in mononuclear TM complexes with ligands ER for different R groups.

3.1. Complexes with ligands BF, BO^- and BNH_2

It has long been speculated that TM complexes with the BF ligand, which is isoelectronic with CO, may become isolable [8]. Recent theoretical studies examined the bonding situation in the complexes $(CO)_nTM(BF)$, $(CO)_nTM(BO^-)$, $(CO)_nTM(BNH_2)$ for TM = Cr, Mn^+, Fe, Co^+, and Ni using gradient-corrected DFT calculations and the ETS energy partitioning scheme [9–11]. The results were compared with the carbonyl complexes $TM(CO)_{n+1}$. Table 1 shows the calculated bond energies of the $(CO)_nTM$–BR bond and the energy partitioning into a term comprizing electrostatic attraction, Pauli repulsion and preparation energy ($\Delta E° + \Delta E_{prep}$) and the attractive orbital interactions (ΔE_{orb}). The latter term is divided into the $RB \rightarrow TM(CO)_n$ σ-donation ΔE_σ and the $RB \leftarrow TM(CO)_n$ π-back-donation ΔE_π.

The calculations predict that the trend of the metal–ligand bond dissociation energies (BDEs) for the ligands AB has the order: $CO < BF < BNH_2 < BO^-$. The boron ligands are more strongly bonded than CO. Please note that the BDEs of the complexes $(CO)_5Mn(BO)$ and $(CO)_4Co(BO)$ are given for dissociation into $(CO)_nTM^+ + BO^-$ and not for dissociation into the energetically lower lying neutral fragments. This explains the very large values for the BDE. The authors say that the difficulty in isolating the complexes $(CO)_nTM(BR)$ is not caused by weak TM–BR bonds, but rather by the high polarity of the BR ligands and the build-up of positive charge at boron, which suggests a low kinetic stability [9,11]. The B–R π* LUMO has a large coefficient at boron and thus becomes susceptible to orbital-controlled nucleophilic attack. The authors suggest that a stabilization of borylene complexes may either be achieved by more steric R groups, or by electronic stabilization in binuclear complexes. The former prediction has been confirmed experimentally by the synthesis of $(CO)_4Fe$–BCp* [3] and $(CO)_4W$–$BN(SiMe_3)_2$ [4].

The partitioning of the orbital interaction energies into ΔE_σ and ΔE_π gives insight into the differences of the bonding situation between the TM–CO and TM–BR

Table 1
Calculated bond dissociation energies (BDE) and energy decomposition (kcal mol^{-1}) at the NL-DFT level[a]

AB		$[Cr(CO)_5(AB)]$	$[\{Mn(CO)_5\}^+AB]$	$[Fe(CO)_4(AB)]$	$[\{Co(CO)_4\}^+AB]$	$[Ni(CO)_3(AB)]$
CO	BDE	−41.8	−44.2	−48.4	−37.3	−28.2
	$\Delta E°+\Delta E_{prep}$	30.5	28.7	38.1	43.8	32.9
	ΔE_σ	−33.8	−43.2	−44.8	−51.8	−28.0
	ΔE_π	−38.5	−29.7	−41.7	−29.3	−33.1
BF	BDE	−62.1	−71.4	−73.8	−70.6	−45.3
	$\Delta E°+\Delta E_{prep}$	38.9	36.8	54.2	63.4	20.0
	ΔE_σ	−59.0	−75.8	−81.7	−100.1	−38.8
	ΔE_π	−42.0	−32.4	−46.3	−33.9	−34.5
BNH_2	BDE	−72.1	−94.4	−87.7	−98.6	−52.7
	$\Delta E°+\Delta E_{prep}$	31.6	20.0	42.2	41.4	17.6
	ΔE_σ	−67.1	−86.2	−89.6	−110.0	−40.9
	ΔE_π	−36.6	−28.2	−40.3	−30.0	−29.4
BO^-	BDE	−93.4	−206.1	−106.1	−216.6	−70.0
	$\Delta E°+\Delta E_{prep}$	−3.2	−88.9	26.2	−54.0	−0.8
	ΔE_σ	−75.6	−101.9	−112.2	−141.5	61.1
	ΔE_π	−14.6	−16.1	−20.1	−21.1	−8.1

[a] Taken from Ref. [11].

bonds (Table 1). As a starting point, we point out that ΔE_σ and ΔE_π have about the same magnitude in the neutral carbonyl complexes $TM(CO)_n$. The energy contribution of the OC ← TM π-backdonation is even stronger than the OC → TM σ-donation in $Cr(CO)_6$ and $Ni(CO)_4$. This is a well known result which has been found in other theoretical studies of TM carbonyls [26,27]. The relative importance of ΔE_σ for the TM–CO bond increases in the positively charged species. This is also in agreement with other theoretical work [27].

Comparison of the bonding contributions to the TM–CO and TM–BR bonds shows the remarkable result that the π-bonding contributions of the neutral ligands CO, BF and BNH_2 are nearly the same (Table 1). The maximum difference is found between $(CO)_4FeB(NH_2)$ ($\Delta E_\pi = -40.3$ kcal mol^{-1}) and $(CO)_4FeBF$ ($\Delta E_\pi = -46.3$ kcal mol^{-1}). However, the contribution of ΔE_σ is clearly the dominant term of the orbital interaction energy for the TM–BR bonds. The ratio $\Delta E_\sigma/\Delta E_\pi$ increases in the order $CO < BF < BNH_2 < BO^-$. This can be explained with the shapes and particularly the energy levels of the frontier orbitals of CO and BR, which are shown in Fig. 2. The energy of the 5σ HOMO increases strongly in the given order, while that of the 2π LUMO of the neutral ligands becomes only slightly lower in energy. This explains why the ΔE_π values for the neutral ligands AB = CO, BF and BNH_2 in the complexes $(CO)_nTM$–AB change very little (Table

1). The increase in the π-donor strength of R in the ligands BR $F < NH_2 < O^-$ yields only a small lowering of the TM–ER π-bond strength given by the ΔE_π values. It becomes obvious that the increase in the TM–AB bond dissociation energies $CO < BF < BNH_2 < BO^-$ is mainly due to the larger contribution of the σ-orbital interactions ΔE_σ and, in some cases, to the change in $\Delta E^\circ + \Delta E_{prep}$. Unfortunately, the authors do not report the contributions of the electrostatic interactions ΔE_{elst} to TM–ER bonding [9–11]. Fig. 2 also shows the frontier orbital energy levels of N_2. The low-lying HOMO of N_2 suggests that the metal–ligand bond energy of dinitrogen complexes should be lower than the BDE of the other ligands. This is indeed the case. The calculated bond energy of $(CO)_4Fe–N_2$ is significantly lower than the BDEs of $(CO)_4Fe–CO$ and $(CO)_4Fe–BF$ [10].

An interesting prediction is made [10,11] about the shift of the B–R stretching frequency when free BR (R = F, NH_2, O^-) becomes a ligand in the complexes $(CO)_5Cr(BR)$. The calculations show that the B–R mode is shifted towards higher wavenumbers by about 100 cm^{-1} [11]. This is opposite to the shift of the C–O stretching frequency in $Cr(CO)_6$, which is calculated to be 153 cm^{-1} lower than in free CO. The authors explain the shift towards higher wavenumbers in the borylene

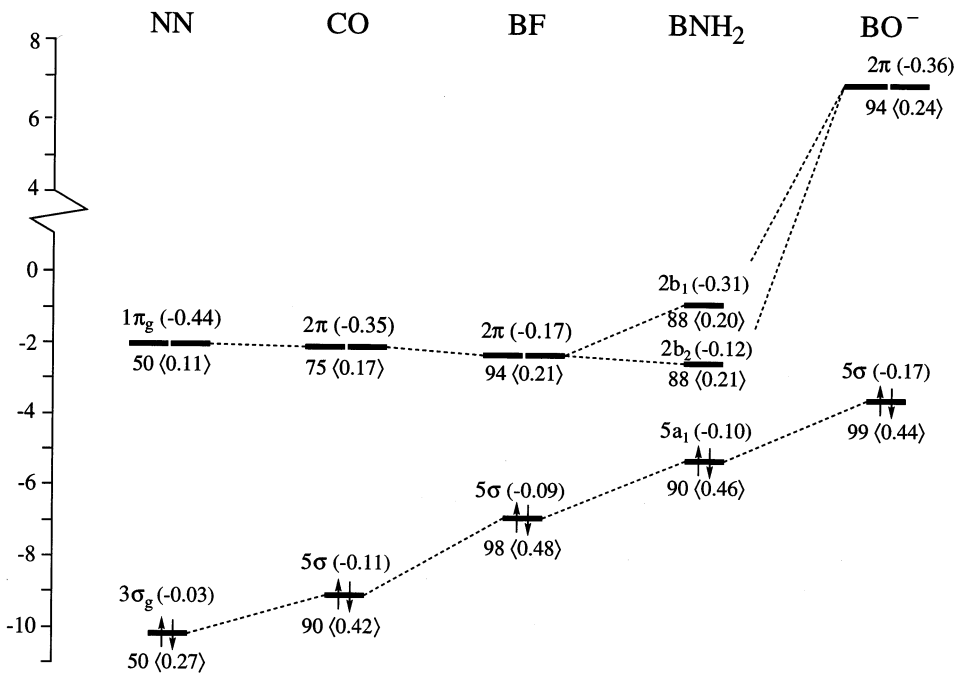

Fig. 2. Frontier orbital energies (eV) of ligands AB. Below each level the percentage of atom A character is given and the overlaps with the relevant $Fe(CO)_4$ frontier orbital are quoted in angular brackets ⟨⟩. Above each level the Mulliken overlap population is given in parentheses. Reproduced with permission from Ref. [11].

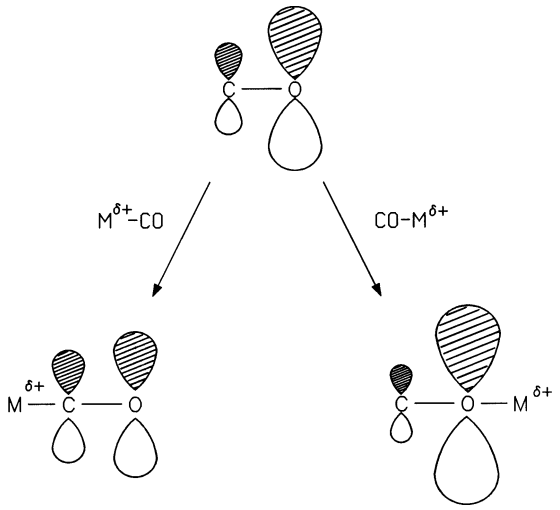

Fig. 3. Effect of a positive charge attached to CO: (a) at the carbon end, which strengthens the CO covalent bond; (b) at the oxygen end, which weakens the CO covalent bond. For details see Reference [29a].

complexes by the nature of the 5σ HOMO of BR, which is said to be antibonding. The antibonding nature is supported by the Mulliken population analysis, which gives a negative B–R overlap population for the 5σ HOMO of BR (Fig. 2). Because the RB→Cr σ-donation is much stronger than the RB←Cr π-backdonation, depopulation of the antibonding 5σ HOMO yields a stronger BR bond in the complex. The opposite effect found for the C–O stretching mode is explained with OC←Cr π-backdonation, which leads to a significant population of the CO 2π* orbitals and thus, to a weaker C–O with a lower stretching frequency than free CO [11]. OC→Cr σ-donation is less important, because the energy level of the 5σ HOMO of CO is lower than that of BF (Fig. 2). However, Fig. 2 shows that the Mulliken population analysis also gives a negative population for the $3\sigma_g$ HOMO of N_2, which corresponds to the 5σ HOMO of BR. σ-only interactions like in H^+–NN lead to a lower N–N stretching frequency than in N_2, which contradicts the alleged antibonding nature of the HOMO at least in N_2.

There is an alternative explanation which has recently been given for the higher C–O stretching frequencies that are found in σ-only ('nonclassical' [28]) TM carbonyl complexes [29]. A positive charge at the carbon end will lead to a change in the polarization of the C–O σ and π orbitals such that the coefficients at C become larger and those at O become smaller than in free CO. This enhances the covalent bond strength of CO and leads to a shorter C–O bond and a higher stretching frequency [29]. The opposite effect is found when the positive charge is attached to the oxygen end, which leads to a longer C–O bond and a lower wavenumber. This is schematically shown in Fig. 3. The latter effect shows that the explanation using an alleged antibonding σ HOMO for CO [9,30] is not plausible,

because it should always give a shorter C–O bond when the positive charge is at the carbon or the oxygen end. The same reasoning may be valid for BR, which should be tested by calculating the B–R stretching frequency in the isomers $(CO)_5CrRB$ [31][2].

Another theoretical study of the authors using the same methods as above compared the bonding of BF with N_2, CO and SiO in $(CO)_4Fe(ER)$ and in the homoleptic complexes $Fe(ER)_5$ [10]. The same conclusion was reached about TM–BF bonding as in the previous work [9,11]. BF has a higher Fe–ER bond energy than N_2, CO and also SiO in the homoleptic complexes $Fe(ER)_5$. Unlike N_2 and SiO, BF shows a slight preference for the equatorial position over the axial site in $(CO)_4Fe(BF)$ [10].

3.2. Complexes $(CO)_5W$–AlR and $(CO)_5W$–$AlR(NH_3)_2$ (R = H, Cl)

Most theoretical studies of TM complexes with Group 13 ligands ER focused on ligands where R is a π-donor ligand. Quantum chemical calculations of borylene complexes showed that complexes with ligands BR where R carries a p(π) electron lone-pair become kinetically stabilized by $R \rightarrow B$ π-donation [9–11]. Indeed, the only stable borylene complexes that have been synthesized so far have BR ligands where R is a strong π-donor (Cp* [3] and $N(SiMe_3)_2$ [4]). The situation is different for the heavier diyl analogs ER (E = Al–Tl), where stable complexes have been isolated with bulky R ligands which are not strong π donors. Examples will be given below.

A recent combined experimental/theoretical study by Fischer, Frenking and co-workers [15] addressed the question of the differences in the bonding situation between $(CO)_5W$–AlH and $(CO)_5W$–AlCl alanediyl complexes, and the changes in the electronic structure when the diyl ligands become additionally stabilized by two molecules of ammonia in $(CO)_5W$–$AlR(NH_3)_2$. Examples for the latter species with tmeda instead of $2NH_3$ are experimentally known and have been characterized spectroscopically and by X-ray structure analysis [15], while the former species without a base could not be isolated. The analysis of the bonding situation gave surprising results. Fig. 4 shows the optimized geometries of the four alanediyl complexes and the theoretically predicted bond dissociation energies D_e which were calculated at the MP2 theory level using a relativistic ECP for tungsten. Table 2 gives the most important results about the electronic structure and bonding situation obtained from the CDA and NBO partitioning schemes.

The analysis of the bonding situation can be summarized as follows [15]. The complexes with the base-free ligands $(CO)_5W$–AlR have clearly shorter W–Al bonds than the complexes with additional ammonia $(CO)_5W$–$AlR(NH_3)_2$, but the W–Al bond dissociation energies of the latter are much higher than those of the

[2] The bond lengthening of COH^+ could be explained in terms of orbital interactions between OC and H^+ if it is assumed that the empty 1s AO of H^- interacts mainly with lower lying bonding σ orbitals of CO and not with the alleged antibonding 5σ HOMO. However, this is not a convincing argument because the other occupied σ orbitals of CO are much lower in energy than the HOMO.

Table 2
Calculated W–Al bond dissociation energies D_e (kcal mol^{-1}), NBO and CDA data of $(CO)_5$–WAlR and $(CO)_5$–WAlR$(NH_2)_3$ (R = H, Cl) at MP2[a,b]

Molecules	D_e	q (W(CO)$_5$)	q (W)	q (Al)	P (W–Al)	d (Al → W)	b (Al ← W)	d (H_3N → Al)	b (H_3N ← Al)
$(CO)_5WAlH$	70.0	−0.64	−0.93	1.07	0.60	0.399	0.301	–	–
$(CO)_5WAlCl$	58.4	−0.58	−0.94	1.13	0.59	0.370	0.301	–	–
$(CO)_5WAlH(NH_3)_2$	100.9	−0.93	−0.67	1.09	0.37	0.474	0.271	0.643	0.069
$(CO)_5WAlCl(NH_3)_2$	93.1	−0.90	−0.72	1.24	0.40	0.356	0.280	0.679	0.056

[a] Taken from Ref. [15].
[b] Partial charges q, Wiberg bond indices P, charge donation d and backdonation b.

former. The explanation for the longer and yet stronger W–Al bonds in $(CO)_5W–AlR(NH_3)_2$ was given in terms of the hybridization of the σ lone-pair orbital at aluminum, which serves as the donor orbital. The Al lone-pair orbital of the tricoordinated $AlR(NH_3)_2$ ligands has a much higher percentage p-character (lower percentage s-character) than AlR (Table 2). The higher percentage s-character makes the lone-pair orbitals in AlH and AlCl more compact and energetically lower than the more diffuse and energetically higher Al lone-pair orbitals in $AlR(NH_3)_2$. This means that the orbital interactions between the HOMO of AlR and LUMO of $W(CO)_5$ take place at shorter interatomic distances but are less stabilizing than the $(CO)_5W–AlR(NH_3)_2$ donor–acceptor interactions [15].

Table 2 shows that the W–Al bonds are thermodynamically very strong even in the 'naked' W–AlR complexes. The calculated bond dissociation energy of $(CO)_5W–AlH(NH_3)_2$ ($D_e = 100.9$ kcal mol^{-1}) places the W–Al bond as one of the

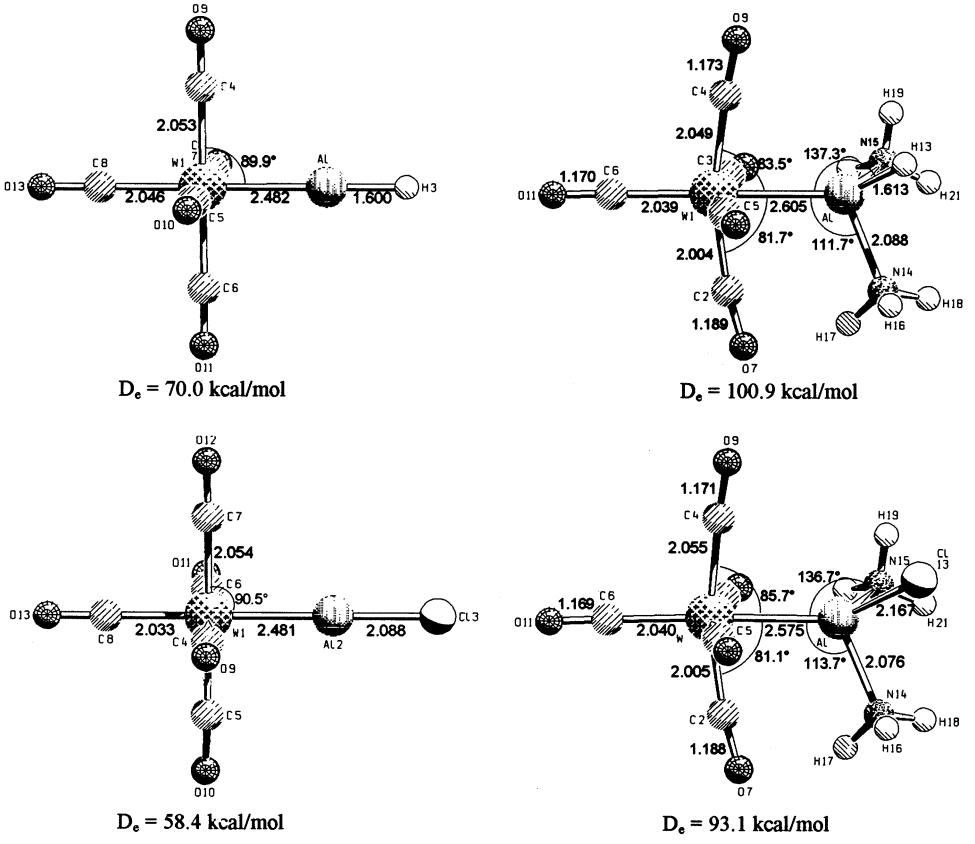

Fig. 4. Optimized geometries and theoretically predicted W–Al bond dissociation energies calculated at the MP2 level. Bond lengths are given in angstroms, bond angles in degrees. Reproduced with permission from Ref. [15].

Table 3
Calculated W–E bond dissociation energies D_e (kcal mol^{-1}), NBO and CDA data of $(CO)_5$–W–ECl$(NH_3)_2$ at MP2[a,b]

Molecules	D_e	q (W(CO)$_5$)	q (W)	q (E)	P (W–E)	d (E→W)	b (E←W)
$(CO)_5$WBCl$(NH_3)_2$	119.6	−0.63	−0.53	0.19	0.42	0.196	0.095
$(CO)_5$WAlCl$(NH_3)_2$	93.1	−0.90	−0.72	1.24	0.40	0.356	0.280
$(CO)_5$WGaCl$(NH_3)_2$	70.9	−0.72	−0.73	1.07	0.44	0.434	0.213
$(CO)_5$WInCl$(NH_3)_2$	70.5	−0.77	−0.71	1.18	0.42	0.449	0.207
$(CO)_5$WTlCl$(NH_3)_2$	47.8	−0.61	−0.70	1.08	0.42	0.411	0.114

[a] Taken from Ref. [15].
[b] Partial charges q, Wiberg bond indices P, charge donation d and backdonation b.

strongest donor–acceptor bonds between a ligand and a transition metal fragment in a neutral TM complex. The CDA results shown in Table 2 suggest that the W–Al binding interactions have large contributions from W→Al π-backdonation. Note the difference between the W–Al and Al–NH_3 bonds: the latter does not show significant H_3N←Al π-backdonation, because there are no low lying π-acceptor orbitals at nitrogen. It is interesting to see that $(CO)_5$W–AlH and $(CO)_5$W–AlCl have similar W→Al π-backdonation. The differences between R = H and R = Cl become larger when ammonia becomes attached, but W→Al π-backdonation remains important. Table 2 shows also that there is large charge transfer from the alanediyl ligand to the tungsten carbonyl in $(CO)_5$W–AlR which becomes even larger in $(CO)_5$W–AlR$(NH_3)_2$. The conclusion about the nature of the W–Al bonds in the base-free and base-supported alanediyl complexes was, that it has a strong ionic character and that the covalent part of the binding interactions has a significant contribution from W→Al π-backdonation. Cl→Al π-donation appears to be less important in the alanediyl complexes than the R→B π-donation in borylene complexes discussed above. The strong ionic character of the W–Al bonds is also revealed by the rather low values of the Wiberg bond indices P(W–Al) (Table 2). According to the bond order, the covalent contributions to the W–Al interactions are less than a single bond.

3.3. Complexes $(CO)_5$W–ECl$(NH_3)_2$ (E = B–Tl)

The same experimental/theoretical study discussed above also gave the results for the whole set of Group 13 base-supported complexes $(CO)_5$W–ECl$(NH_3)_2$ (E = B, Al, Ga, In, Tl) which makes it possible to study the trends in the structure and bonding interactions for the different atoms E. Table 3 shows the theoretically predicted bond energies of the W–E bond at the MP2 theory level and the most important results of the NBO and CDA calculations.

The W–E bond energies given in Table 3 show the trend B > Al > Ga ~ In > Tl. It will be seen that the same trend is predicted for all investigated complexes

L_nTM–ER which have been studied so far. The trend in the bond order is the same for different transition metals TM of Groups 6, 8 and 10 with different R subsituents.

The charge distribution given by the NBO method indicates a significant charge donation from the ligands $ECl(NH_3)_2$ to the $W(CO)_5$ fragment. The largest charge donation is found for the aluminum complex (-0.90 e), and the smallest values are calculated for the thallium (-0.61 e) and boron complexes (-0.63 e). In all the complexes studied, the tungsten atom carries a large negative charge, while the Group 13 elements have a high positive charge $> +1.0$ with the exception of boron. The atomic partial charges thus suggest that the W–E bonds are mainly ionic, with the possible exception of the W–B bond. A low covalent contribution to the W–E bonds is also indicated by the Wiberg bond indices, which are < 0.5 for all elements E. The CDA results suggest that the $E \rightarrow W$ σ-donation is always larger than the $E \leftarrow W$ π-backdonation, which is in agreement with the calculated charge distribution.

3.4. Complexes $(CO)_4Fe$–ECp (E = B–Tl)

Until 1997, all experimentally known TM complexes with Group 13 diyl ligands ER that were unquestionably characterized by spectroscopic means had additional bases attached to the ligands ER [1,31]. The first base-free Group 13 diyl complex was reported by Fischer et al. [2] who synthesized $(CO)_4Fe$–AlCp*. The analogous Ga [32] and boron complexes [3] have in the meantime also been isolated. The remarkable experimental achievements led to theoretical studies that analyzed the bonding situation in the complexes $(CO)_4Fe$–ECp (E = B–Tl) at the non-local DFT level [2,16]. The central question about the Fe–ECp interactions was about the strength of the $Fe \rightarrow ECp$ π-backdonation, because the formally empty p(π) orbitals at E should receive significant electronic charge from the Cp ligand. Fig. 5 shows the theoretically predicted geometry of $(CO)_4Fe$–AlCp at BP86, which is in good agreement with the experimental values for $(CO)_4Fe$–AlCp* [2]. The calculated geometries of the other Group 13 complexes $(CO)_4Fe$–ECp are similar to the aluminum complexes except for E = Tl, where the center of the Cp ring does not lie on the Fe–Al axis (Fig. 5). The Tl–C(Cp) distances vary considerably between 2.508 and 2.958 Å, which indicates that the thallium atom is not η^5-bonded to the Cp ring.

The most important results of the bonding analysis are shown in Table 4. There is strong Coulomb attraction between the negatively charged Fe and the positively charged atoms E. The large ionic character of the Fe–E bonds is also revealed by the low values of the Wiberg bond indices P(Fe–E) < 0.5. The changes in the σ and π charges $\Delta q_\sigma(E)$ and $\Delta q_\pi(E)$ suggest that there is significant $E \rightarrow Fe$ σ-donation but less $E \leftarrow Fe$ π-backdonation in the complexes. This is supported by the results of CDA calculations, which shows that the $E \rightarrow Fe$ σ-donation is clearly stronger than the $E \leftarrow Fe$ π-backdonation, although the latter is not negligible. The $E \rightarrow Fe$

Table 4
Calculated Fe–E bond dissociation energies D_e (kcal mol^{-1}), NBO and CDA data of $(CO)_4$–Fe–ECp at BP86[a,b]

E	Isomer	D_e	q (Fe(CO)$_4$)	q (Fe)	q (E)	p_x (E)[c]	p_y (E)[c]	p_z (E)	Δq_π (E)[f]	Δq_σ (E)[f]	P (Fe–E)	P (Fe–CO)[d]	d (CpE → Fe)	b (CpE ← Fe)
Complexes $(CO)_4$–Fe–Ecp														
B	ax	77.99	−0.51	−0.56	0.32	0.51	0.51	0.71	−0.40	+0.67	0.48	0.70	0.598	0.277
Al	ax	53.12	−0.67	−0.58	1.18	0.29	0.29	0.26	−0.30	+0.89	0.48	0.69	0.401	0.188
Ga	ax	32.89	−0.46	−0.51	0.96	0.27	0.27	0.21	−0.24	+0.61	0.49	0.77	0.413	0.039
In	ax	33.86	−0.53	−0.49	1.06	0.25	0.25	0.19	−0.19	+0.64	0.48	0.78	0.361	0.187
Tl	eq	17.11	−0.30	−0.51	0.81	–	–	–	–	–	0.32	0.73	0.240	0.063
Free ligands ECp[e]														
B					0.05	0.31	0.31	0.69						
Al					0.59	0.14	0.14	0.26						
Ga					0.59	0.15	0.15	0.18						
In					0.61	0.15	0.15	0.18						
Tl					0.63	0.15	0.16	0.10						

[a] Taken from Ref. [16].
[b] Partial charges q, p orbital population, difference of the π-charges and the σ-charges of the atom E between the complexes and the free ligands Δq_π and Δq_σ, Wiberg bond indices P, charge donation d and backdonation b.
[c] p(π) AO of atom E.
[d] CO_{ax} *trans* to ECp; CO_{eq} in case of the equatorial isomer.
[e] Calculated using the frozen geometries in the complexes.
[f] A negative number indicates higher electronic charge and a positive number indicates less electronic charge in the complex than in the free ligand.

σ-donation is largely caused by the frontier orbital interaction between the HOMO of ECp (lone-pair MO at E) and the LUMO of $Fe(CO)_4$. This is shown for $(CO)_4Fe$–AlCp in Fig. 6. However, the low covalent bond order suggests that the covalent contributions to the Fe–E bonds are much less important than the coulombic interactions. Please note that the changes in the partial charges $q(E)$ between the free ligands and the complexes do not indicate the rather large alterations in the charge distribution, which is only revealed by the substantial changes in the σ and π charges (Table 4).

The ligands ECp are more energetically favored (by less than 1 kcal mol^{-1}) in the axial position than in the equatorial position except for E = Tl, where the equatorial form is 0.4 kcal mol^{-1} lower in energy than the axial form [16]. Optimization of the borylene complex gave only the axial isomer as the minimum

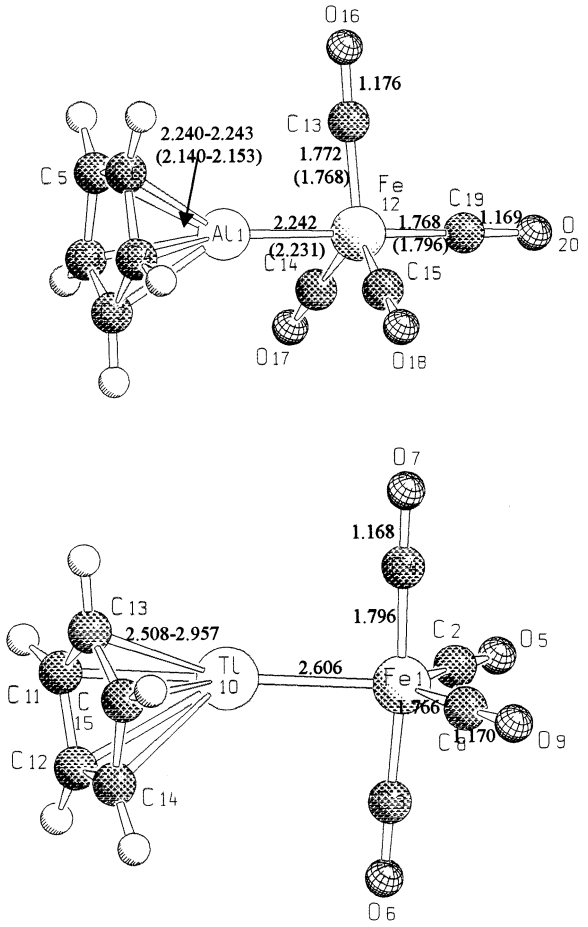

Fig. 5. Calculated geometries of $(CO)_4FeAlCp$ and $(CO)_4FeTlCp$ at BP86. Bond lengths are given in angstroms, bond angles in degrees. Reproduced with permission from Ref. [16].

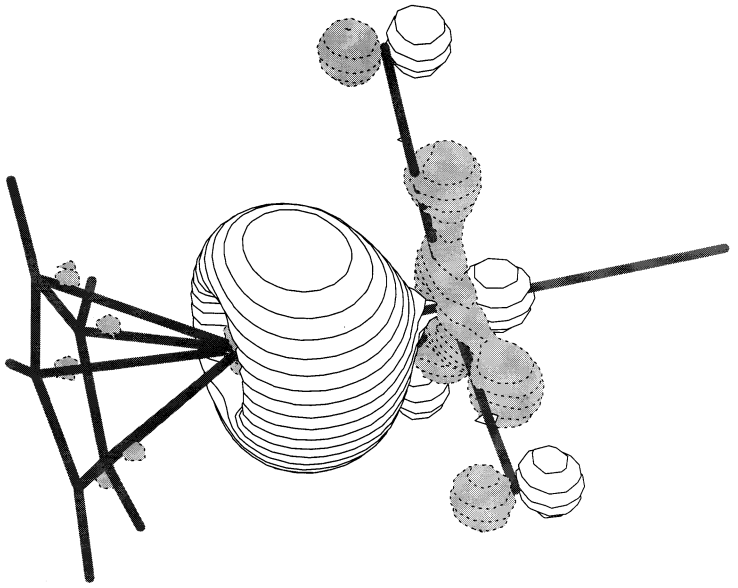

Fig. 6. Molecular orbital of $(CO)_4FeAlCp$ which shows the dominant contribution of the Al→Fe electron donation according to the CDA results. Reproduced with permission from Ref. [2].

energy structure [16]. The calculated preference of the axial isomer for the Al and Ga complexes is in agreement with experimental evidence [2,3,32]. The BP86 calculations predict that the $(CO)_4Fe$–ECp bond strength trend is in the order B > Al > Ga ~ In > Tl. This is the same trend as for $(CO)_5W$–$ECl(NH_3)_2$ (Table 3). The absolute values for the bond strengths of the latter complexes are much higher than for the former. However, the bond energies of $(CO)_5W$–$ECl(NH_3)_2$ were calculated at the MP2 level [15], which is known to give bond energies for donor–acceptor bonds that are too high [19a]. Thus, the absolute values of the bond energies obtained with the two methods BP86 and MP2 should not be compared.

3.5. Complexes $(CO)_4Fe$–$EN(SiH_3)_2$ and $(CO)_5W$–$EN(SiH_3)_2$ (E = B–Tl)

The first experimentally characterized borylene complexes with an amino group attached to boron are $(CO)_4Fe$–$BN(SiMe_3)_2$ and $(CO)_5W$–$BN(SiMe_3)_2$, which have only recently been isolated [4]. Earlier reports about the synthesis of $(CO)_4Fe$–$BNMe_2$ [33] are probably not correct [4,31]. The geometry of the tungsten complex has been measured by X-ray structure analysis, while $(CO)_4Fe$–$BN(SiMe_3)_2$ was spectroscopically identified [4]. The higher homologues of complexes with the ligand ENR_2, where E = Al–Tl, are experimentally unknown. The bonding situation in borylene complexes with BNH_2 ligands has been investigated with quantum chemical methods by Ehlers et al. [9]. The results are discussed in Section 3.1. Another recent theoretical study analyzed the bonding situation for

all Group 13 elements in the $(CO)_4Fe–EN(SiH_3)_2$ and $(CO)_5W–EN(SiH_3)_2$ (E = B–Tl) complexes at the BP86 theory level [16]. The most important results shall briefly be discussed.

Fig. 7 shows the theoretically predicted geometries of $(CO)_4Fe–BN(SiH_3)_2$ and $(CO)_5W–BN(SiH_3)_2$. The latter structure is in good agreement with the X-ray structure analysis of $(CO)_5W–BN(SiMe_3)_2$ [4]. A remarkable theoretical prediction is the equatorial position of the $BN(SiH_3)_2$ ligand in $(CO)_4Fe–BN(SiH_3)_2$. Geometry

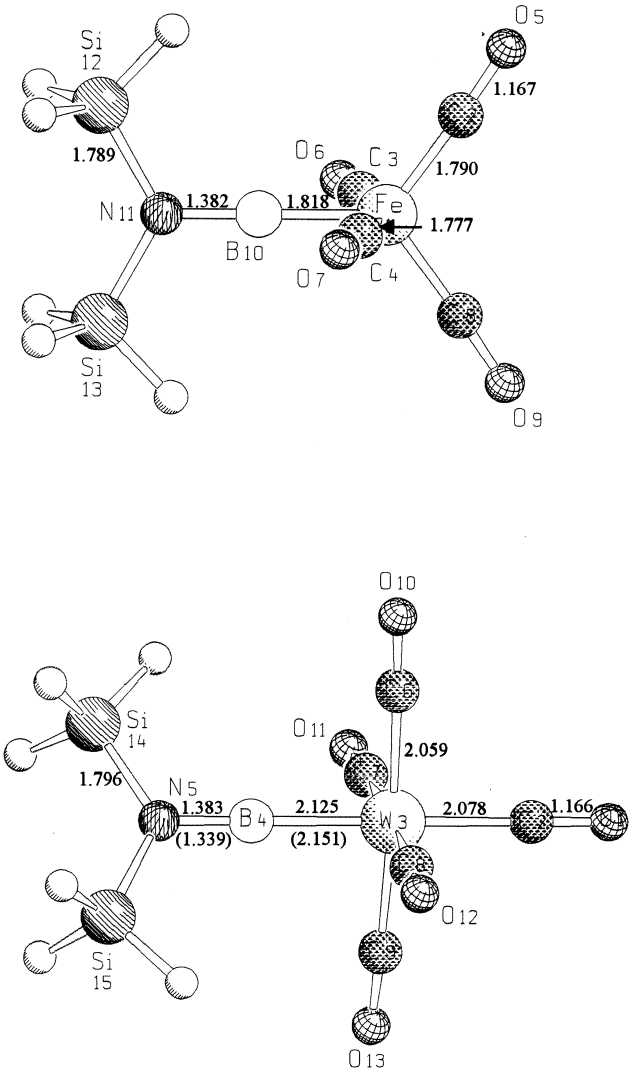

Fig. 7. Calculated geometries of $(CO)_4FeBN(SiH_3)_2$ and $(CO)_5WBN(SiH_3)_2$ at BP86. Bond lengths are given in angstroms, bond angles in degrees. Experimental bond lengths from Ref. [4] are given in parentheses. Reproduced with permission from Ref. [16].

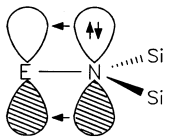

Fig. 8. Schematic representation of the dominant intraligand N → E π-donation in $EN(SiH_3)_2$.

optimization of the axial isomer gave only the equatorial form as the minimum energy structure. This is different from the situation in $(CO)_4Fe$–BCp, where both isomeric forms are energy minima, the axial isomer being slightly lower in energy than the equatorial form. The experimental study about the synthesis of $(CO)_4Fe$ $BN(SiMe_3)_2$ did not give information about the position of the borylene ligand [4]. Geometry optimization of the heavier Group 13 homologues of $(CO)_4Fe$ $BN(SiH_3)_2$ (E = Al, Tl) gave axial and equatorial forms as equilibrium structures. The equatorial isomer of the Al complex was 1.1 kcal mol^{-1} lower in energy than the axial form, while the axial isomers of E = Ga, In and Tl were slightly (0.2–0.7 kcal mol^{-1}) more stable than the equatorial forms [16].

Table 5 gives the most important results taken from the analysis of the bonding situation in $(CO)_4Fe$–$EN(SiH_3)_2$ and $(CO)_5W$–$EN(SiH_3)_2$. The Fe–$EN(SiH_3)_2$ bond dissociation energies are slightly higher than the W–$EN(SiH_3)_2$ bond energies (except for the nearly identical values for E = Tl) and similar in magnitude to the bond energies of the Fe–ECp complexes (Table 4). The trend seen for the bond energies is in all cases B > Al > Ga ~ In > Tl. The Fe–E and W–E bonds are very polar and are held together mainly by strong charge attraction between the negatively charged TM and the positively charged Group 13 element. The Wiberg bond indices P(TM–E) are slightly higher than in the cases discussed above, but are still less than the values for a single bond.

The CDA results suggest that there are strong E → TM σ-donation and weaker, but significant E ← TM π-backdonation in the complexes. This is in agreement with the interpretation of the bonding situation in $(CO)_5W$–$BN(SiMe_3)_2$ that was made based on the IR spectrum of the compound [4]. The ratio of E → Fe donation and E ← Fe backdonation shows that there is a higher degree of backdonation in $(CO)_4Fe$–$EN(SiH_3)_2$ (Table 5) than in $(CO)_4Fe$–ECp (Table 4). The noticeable E ← Fe π-backdonation is also indicated by the population of the p(π) orbitals at E. The calculated Δq_π(E) values (Table 5) suggest that there is a particularly strong E ← Fe backdonation when E = B, Al. The CDA and NBO results both suggest that E ← TM backdonation in $(CO)_4Fe$–$EN(SiH_3)_2$ is stronger than in $(CO)_5W$–$EN(SiH_3)_2$ (Table 5). The p(π) acceptor orbitals at E in $EN(SiH_3)_2$ are not equivalent because the substituent has C_{2v} symmetry (Fig. 8).

A remarkable result of the NBO population analysis is that the in-plane p(π) AO of atom E, which is nearly empty in the free ligands $EN(SiH_3)_2$, becomes significantly occupied via E ← Fe π-backdonation in the complexes. In the boron and aluminum complexes it is even more populated than the out-of-plane p(π) orbital (Table 5). The trend of the E ← Fe π-backdonation given by the Δp(π) values of the

Table 5
Calculated TM–E bond dissociation energies D_e (kcal mol^{-1}), NBO and CDA data of $(CO)_4$–Fe–$EN(SiH_3)_2$ and $(CO)_5$–W–$EN(SiH_3)_2$ at BP86[a,b]

E	Isomer	D_e	q (TM(CO)$_{4/5}$)	q (TM)	q (E)	p_x (E)[c]	p_y (E)[d]	p_z (E)	Δq_π (E)[g]	Δq_σ(E)[g]	P (TM–E)	P (TM–CO)[e]	d (E→TM)	B (E←TM)
Complexes $(CO)_4$–Fe–$EN(SiH_3)_2$														
B	eq	85.83	−0.31	−0.58	0.59	0.39	0.48	0.61	−0.60	+0.68	0.65	0.62	0.583	0.476
Al	eq	52.98	−0.57	−0.63	1.23	0.20	0.30	0.21	−0.37	+0.81	0.51	0.63	0.368	0.208
Ga	ax	39.68	−0.53	−0.56	1.14	0.24	0.20	0.19	−0.31	+0.69	0.53	0.71	0.393	0.128
In	ax	38.92	−0.57	−0.53	1.21	0.21	0.17	0.16	−0.27	+0.70	0.50	0.73	0.214	0.165
Tl	ax	25.35	−0.46	−0.48	1.07	0.18	0.14	0.13	−0.21	+0.49	0.44	0.79	0.243	0.079
Free ligands $EN(SiH_3)_2$[f]														
B					0.51	0.21	0.06	0.57						
Al					0.79	0.11	0.02	0.23						
Ga					0.76	0.11	0.02	0.23						
In					0.78	0.10	0.01	0.22						
Tl					0.79	0.10	0.01	0.20						
Complex $(CO)_5$–W–$EN(SiH_3)_2$														
B		75.08	−0.36	−0.87	0.69	0.30	0.31	0.66	−0.34	+0.52	0.82	0.75	0.750	0.329
Al		44.40	−0.61	−0.99	1.30	0.17	0.11	0.23	−0.15	+0.66	0.56	0.84	0.566	0.287
Ga		36.69	−0.54	−0.96	1.20	0.16	0.10	0.21	−0.13	+0.56	0.53	0.87	0.509	0.258
In		36.46	−0.60	−0.93	1.27	0.14	0.08	0.17	−0.11	+0.60	0.50	0.89	0.309	0.186
Tl		25.24	−0.50	−0.86	1.15	0.12	0.07	0.14	−0.08	+0.46	0.44	0.94	0.432	0.155
Free ligand $EN(SiH_3)_2$[f]														
B					0.51	0.21	0.06	0.57						
Al					0.79	0.11	0.02	0.22						
Ga					0.77	0.11	0.02	0.23						
In					0.78	0.10	0.01	0.22						
Tl					0.77	0.10	0.01	0.19						

[a] Taken from Ref. [16].
[b] Partial charges q, p orbital population, difference of the π-charges and the σ-charges of the atom E between the complexes and the free ligands Δq_π and Δq_σ, Wiberg bond indices P, charge donation d and backdonation b.
[c] p(π) AO of atom E which is perpendicular to the Si–N–Si plane.
[d] p(π) AO of atom E which is in the Si–N–Si plane.
[e] CO_{ax} *trans* to $EN(SiH_3)_2$; CO_{eq} in the case of the equatorial isomer.
[f] Calculated using the frozen geometries in the complexes.
[g] A negative number indicates higher electronic charge and a positive number indicates less electronic charge in the complex than in the free ligand.

NBO analysis agree nicely with the CDA results. Thus, both methods suggest relatively strong E←TM π-backdonation. Without the latter, the Group 13 elements would have an electron sextet in the valence shell in the complexes $(CO)_n$TM–ENR_2. However, the dominant contributions to the TM–ENR_2 bonds still arise by the charge attraction between TM and E and not by covalent interactions.

3.6. Complexes $(CO)_4$Fe–EPh (E = B–Tl)

All TM complexes with terminal Group 13 diyl ligands ER which until recently were synthesized had either a π-donor ligand R attached to R, or the TM–ER bond was additionally stabilized by bases such as amines in L_nTM–E$R(NR_3)_n$ [1]. In 1997 Robinson et al. [5] reported the synthesis of $(CO)_4$Fe–GaAr* (Ar* = 2,6-(2,4,6-triisopropylphenyl)-phenyl), which has an unsupported Fe–GaR bond where R is not a strong π-donor. The π-system of the aryl ring might become a weak donor for the out-of-plane p(π) orbital of gallium, but the electron donation should not be strong and the in-plane p(π) AO of Ga would still remain empty (Fig. 9). The large aryl substituent R obviously provides enough steric protection for the electron-deficient EAr* group that makes $(CO)_4$Fe–GaAr* stable enough to become isolated. The question arises, if in the absence of strong Ga←Ar* π-donation does the Ga←Fe π-backdonation become enhanced. If not, gallium would have only four electrons in the valence shell in $(CO)_4$Fe–GaAr*.

Robinson argued that there is substantial Ga←Fe π-backdonation in the complex, because the X-ray structure analysis of $(CO)_4$Fe–GaAr* showed a linear Fe–Ga–C(Ph) arrangement and a rather short Fe–Ga bond [5]. The authors suggested a Fe–Ga triple bond for the complex, which would mean that gallium has an electron octet. The interpretation of a Fe–Ga triple bond was dismissed by Cotton and Feng [13] because (a) a Lewis structure $(CO)_4$Fe≡GaAr* would lead to a formal negative charge at Ga and positive charge at Fe, which was said to be unbelievable; (b) The C–O stretching frequency of the Fe–CO ligands should be shifted towards higher wavenumbers if Ga←Fe π-backdonation is large. This is not the case, the C–O stretching mode is rather low [5]. (c) The Fe–Ga bond should be shorter than the Fe–PR_3 bond, if Ga is indeed a strong π-acceptor [13].

The pro and contra arguments about the alleged Fe≡Ga triple bond have been critically examined in a recent theoretical study by Boehme and Frenking (BF) [14]. BF concluded that none of the arguments in favor or against a bond could be considered as true evidence about the nature of the Fe–Ga bond in

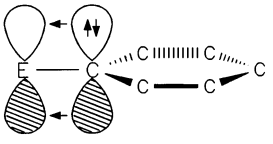

Fig. 9. Schematic representation of the dominant intraligand phenyl→E π-donation in E(Ph). Only one p(π) AO of the phenyl ring is shown.

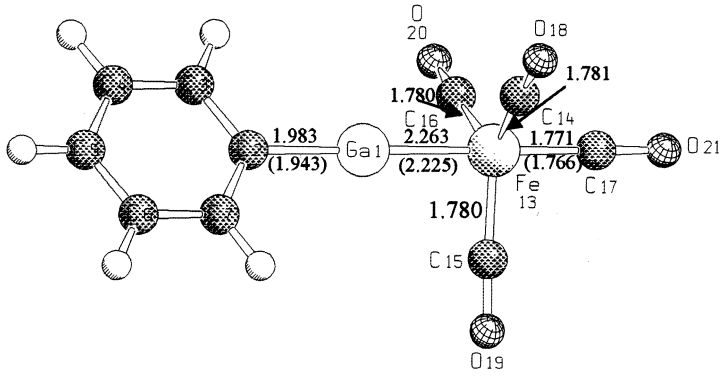

Fig. 10. Calculated geometry of $(CO)_4FeGaPh$ at BP86. Bond lengths are given in Å, bond angles in degree. Experimental bond lengths from Ref. [5] are given in parentheses. Reproduced with permission from Ref. [16].

$(CO)_4Fe$–GaAr*. The authors presented a quantum chemical study at the DFT theory level (BP86) of the structures of $(CO)_4Fe$–Ga(Ph) [14]. They also presented an analysis of the Fe–Ga bonding situation using the CDA and NBO methods. An extension of this work to the other Group 13 elements in the complexes $(CO)_4Fe$–EAr* (E = B–Tl) has recently been given by Uddin, Boehme and Frenking (UBF) [16].

Fig. 10 shows the optimized geometry of $(CO)_4Fe$–Ga(Ph), which is in good agreement with the X-ray structure analysis of $(CO)_4Fe$–GaAr*. Table 6 shows the most important theoretical data which are pertinent to the Fe–E bond. The theoretically predicted Fe–E bond dissociation energies of $(CO)_4Fe$–E(Ph) are significantly higher than the Fe–ER bond energies in complexes where R is a π-donor ligand (Tables 1–5). This indicates enhanced Fe–E(Ph) binding interactions in the complexes. The trend for the Fe–E(Ph) bond energies is the same as for the other Fe–ER bonds where R is a π-donor ligand, i.e. B > Al > Ga ~ In > Tl. The axial isomers are slightly lower in energy than the equatorial forms for the heavier Group 13 elements Ga, In and Tl. For E = Al the two isomers are nearly degenerate in energy, while only the equatorial form of the aminoborylene complex is a minimum on the potential energy surface [16].

The CDA and NBO analyses of the Fe–E(Ph) bonding situation give a clear answer to the question about the Ph(E) ← Fe π-backdonation, which is the highest for each element compared with the other ER ligands. This is revealed by the difference in the p(π) occupation Δq_π(E) between the free ligand E(Ph) and the complex $(CO)_4Fe$–E(Ph), and by the d/b ratio given by the CDA method (Table 6). Both methods show that E(Ph) is the strongest π-acceptor among the ER ligands in the $(CO)_nTM$–ER complexes investigated so far (see Tables 1–6). The ligand $EN(SiH_3)_2$ is nearly as strong a π-acceptor as E(Ph) and yet, the Fe–E(Ph) bond energies are clearly higher than those of the Fe–$EN(SiH_3)_2$ bonds (Tables 5 and 6). Note that the total charge transfer Δq [$Fe(CO)_4$] ← L is always larger when

Table 6
Calculated Fe–E bond dissociation energies D_e (kcal mol^{-1}), NBO and CDA data of $(CO)_4$–Fe–EPh at BP86[a,b]

E	Isomer	D_e	q (Fe(CO)$_4$)	q (Fe)	q (E)	p_x (E)[c]	p_y (E)[d]	p_z (E)	Δq_π (E)[g]	Δq_σ (E)[g]	P (Fe–E)	P (Fe–CO)[e]	d (PhE → Fe)	b (PhE ← Fe)
Complexes $(CO)_4$–Fe–Eph														
B	ax	102.77	−0.36	−0.59	0.65	0.41	0.34	0.65	−0.63	+0.83	0.76	0.57	0.516	0.473
Al	eq	63.60	−0.66	−0.62	1.20	0.15	0.30	0.27	−0.40	+0.87	0.50	0.63	0.399	0.335
Ga	ax	55.03	−0.63	−0.56	1.12	0.21	0.18	0.24	−0.34	+0.76	0.52	0.68	0.383	0.264
In	ax	53.24	−0.67	−0.53	1.16	0.18	0.16	0.23	−0.29	+0.75	0.49	0.70	0.388	0.277
Tl	ax	42.52	−0.60	−0.50	1.04	0.15	0.14	0.19	−0.25	+0.61	0.44	0.74	0.273	0.180
Free ligands Eph[f]														
B					0.45	0.11	0.01	0.69						
Al					0.73	0.05	0.00	0.34						
Ga					0.70	0.05	0.00	0.36						
In					0.70	0.05	0.00	0.36						
Tl					0.68	0.04	0.00	0.36						

[a] Taken from Ref. [16].

[b] Partial charges q, p orbital population, difference of the π-charges and the σ-charges of the atom E between the complexes and the free ligands Δq_π and Δq_σ, Wiberg bond indices P, charge donation d and backdonation b.

[c] p(π) AO of atom E which is perpendicular to the phenyl plane.

[d] p(π) AO of atom E which is in the phenyl plane.

[e] CO_{ax} *trans* to EPh; CO_{eq} in case of the equatorial isomer.

[f] Calculated using the frozen geometries in the complexes.

[g] A negative number indicates a higher electronic charge and a positive number indicates a less electronic charge in the complex than in the free ligand.

L = E(Ph) than when L = $EN(SiH_3)_2$. The high negative charges at Fe and positive charges at E indicate that the Fe–E bond in $(CO)_4$Fe–E(Ph) has substantial ionic character.

The analysis of the bonding situation in $(CO)_4$Fe–Ga(Ph) thus shows that the Ga ← Fe π-backdonation is indeed as important as the Ga → Fe σ-donation, which lends some credence to the formulation with a Fe≡Ga triple bond as suggested by Robinson et al. [5]. Cotton and Feng [13] found that the orbital overlap of π type between iron and gallium in $(CO)_4$Fe–Ga(Ph) is practically nil, but this result was based on a Mulliken population analysis, which is not as reliable as the NBO analysis. However, the sum of the Fe–Ga orbital interactions gives a bond order of only 0.53, which is far from the value expected for a triple bond. It has been pointed out that the tungsten–carbyne bonds in Fischer-type complexes have bond orders between 1.7 and 2.1, and Schrock-type carbyne complexes (alkylidenes) have bond orders between 2.3 and 2.5, which is much closer to triple bond order [25e]. The nature of the Fe–Ga interactions in $(CO)_4$Fe–Ga(Ph) as well as the other Fe–E(Ph) bonds is ionic, and the covalent contributions are much less important. Thus, the classification of $(CO)_4$Fe–GaAr* as a ferrogallyne is not justified. The *relatively* strong (Ph)Ga ← Fe π-backdonation shows, however, that the Group 13 elements try to achieve an 8-electron valence shell.

3.7. Complexes $TM(ECH_3)_4$ (TM = Ni, Pd, Pt; E = B–Tl)

The nickel–indium complex $Ni[InC(SiMe_3)_3]_4$ which was synthesized in 1998 by Uhl et al. [6] was the first example of a homoleptic Group 13 complex that has been isolated and characterized spectroscopically and by X-ray structure analysis. The analogous gallium compound has in the meantime also been synthesized [7]. The bonding situation and the bond strengths in the complexes $TM(ECH_3)_4$ (TM = Ni, Pd, Pt; E = B–Tl) have recently been investigated at the DFT (BP86) theory level using CDA and NBO methods [7,16]. Fig. 11 shows the calculated geometry of the indium complex $Ni(InCH_3)_4$ [7]. The theoretically predicted Ni–In and In–C bond lengths are in good agreement with experimental results. The trend of the TM–E bond dissociation energies shows the familiar order for Group 13 elements B > Al > Ga ~ In > Tl (Table 7). The nickel and platinum complexes have about equal TM–E bond energies, while the palladium species have weaker Pd–E bonds. The TM–EMe bonds are very strong: Even the most weakly bonded Group 13 diyl complex has a stronger $(ER)_3$TM–ER bond than the $(CO)_3$TM–CO bond of the respective TM tetracarbonyl [35].

The pivotal question about the TM–E bond is again if there is substantial RE ← TM π-backdonation to the ligand atoms E, which are not electronically stabilized by E ← R π-backdonation. The NBO and CDA data clearly show that the central atom significantly donates electronic charge into the p(π) orbitals of E. Table 7 gives the calculated data of the population analyses. The p(π) orbitals of E in the free ligands ECH_3 are nearly empty, but they become significantly populated in the complexes. For example, the NBO method suggests that the E ← Ni π-backdonation is between 0.72 e in Ni–BCH_3 and 0.42 e in Ni–$TlCH_3$. The π-backdona-

Table 7
Calculated TM–E bond dissociation energy D_e (kcal mol^{-1}), NBO and CDA data of $TM(ECH_3)_4$ at B3LYP[a,b]

E	D_e	q (TM(ER)$_3$)	q (TM)	q (E)	p_x (E)[c]	p_y (E)[c]	p_z (E)	Δq_π (E)	Δq_σ (E)[e]	P (TM–E)[e]	d ($H_3CE \rightarrow TM$)	b ($H_3CE \leftarrow TM$)
Complexes Ni(ECH$_3$)$_4$												
B	83.80	0.04	0.16	0.31	0.39	0.39	0.73	−0.72	+0.55	0.56	0.670	0.482
Al	55.64	−0.10	−0.48	0.76	0.31	0.31	0.33	−0.60	+0.62	0.52	0.597	0.461
Ga	43.15	−0.07	−0.30	0.67	0.26	0.26	0.34	−0.50	+0.47	0.51	0.604	0.410
In	45.44	−0.14	−0.44	0.72	0.29	0.29	0.30	−0.56	+0.57	0.53	0.526	0.384
Tl	28.39	−0.08	−0.30	0.64	0.21	0.21	0.30	−0.42	+0.38	0.52	0.470	0.368
Complexes Pd(ECH$_3$)$_4$												
B	67.46	0.02	0.20	0.30	0.38	0.38	0.73	−0.70	+0.52	0.60	0.680	0.551
Al	46.02	−0.10	−0.50	0.77	0.26	0.26	0.34	−0.50	+0.53	0.44	0.563	0.552
Ga	33.43	−0.11	−0.40	0.70	0.23	0.23	0.35	−0.44	+0.44	0.43	0.541	0.429
In	37.42	−0.18	−0.59	0.77	0.23	0.23	0.30	−0.44	+0.60	0.45	0.432	0.364
Tl	19.88	−0.13	−0.46	0.69	0.17	0.17	0.30	−0.34	+0.35	0.42	0.525	0.329
Complexes Pt(ECH$_3$)$_4$												
B	82.68	0.05	0.35	0.24	0.41	0.41	0.78	−0.76	+0.52	0.68	0.650	0.610
Al	57.32	−0.16	−0.69	0.80	0.29	0.29	0.36	−0.56	+0.62	0.48	0.639	0.551
Ga	43.34	−0.15	−0.60	0.72	0.25	0.25	0.36	−0.48	+0.50	0.47	0.576	0.494
In	46.79	−0.16	−0.81	0.79	0.25	0.25	0.30	−0.48	+0.56	0.48	0.488	0.402
Tl	26.20	−0.13	−0.69	0.71	0.20	0.20	0.29	−0.40	+0.43	0.46	0.508	0.361
Free Ligand ECH$_3$[d]												
B				0.48	0.03	0.03	0.71					
Al				0.74	0.01	0.01	0.37					
Ga				0.70	0.01	0.01	0.40					
In				0.71	0.01	0.01	0.39					
Tl				0.68	0.00	0.00	0.39					

[a] Taken from Ref. [16].

[b] Partial charges q, p orbital population, difference of the π-charges and the σ-charges of the atom E between the complexes and the free ligands Δq_π and Δq_σ, Wiberg bond indices P, charge donation d and backdonation b.

[c] p(π) AO of atom E which is perpendicular to TM–E–C axis.

[d] Calculated using the frozen geometries in the complexes; identical values have been found in the free ligands for all complexes of Ni, Pd and Pt.

[e] A negative number indicates higher electronic charge and a positive number indicates less electronic charge in the complex than in the free ligand.

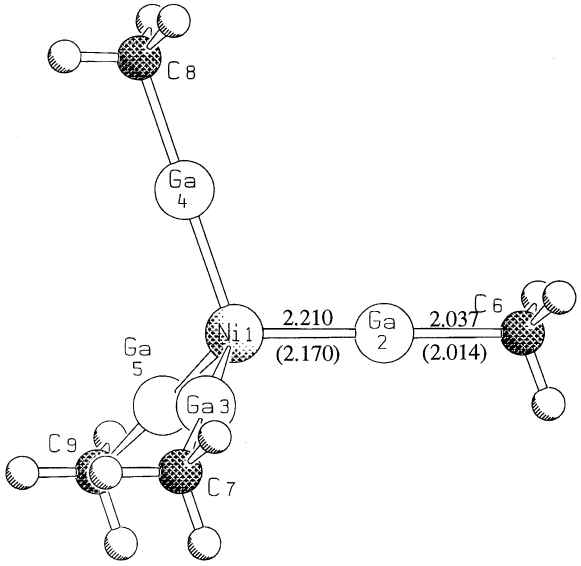

Fig. 11. Calculated bond lengths (Å) of tetrahedral $Ni(InCH_3)_4$ at BP86. Experimental bond lengths from Ref. [6] are given in parentheses. Reproduced with permission from Ref. [16].

tion is particularly large in the Pt complexes, which have expanded d-orbitals due to relativistic effects. The calculated values for the π-donation $\Delta q_\pi(E)$ in $TM(ECH_3)_4$ given by the NBO method are the highest of all the complexes discussed in this review. The CDA results support the assignment of strong π-backdonation in $TM(ECH_3)_4$. The calculated atomic partial charges indicate that the TM–EMe bonds of the heavier Group 13 elements Al–Tl have large ionic contributions to the bond strength. The positive partial charge at boron in $TM(BCH_3)_4$ appears to speak against an ionic character of the TM–B bonds (Table 7). However, the charge distribution at the atoms is highly anisotropic, and strongly attractive charge interactions may exist even between positively charged atoms. For example, the bond between H^+ and CO in HCO^+ has $\sim 50\%$ ionic character, although the carbon atom carries a positive partial charge [29a]. The calculated bond orders suggest that the covalent contributions to the TM–E bonds in $TM(ECH_3)_4$ may not be the dominant binding interactions. The Wiberg indices P(TM–E) are small in all cases which means that charge attraction contributes significantly to the bond energy.

4. Summary

The most important results of the theoretical studies about the chemical bonding in the transition metal complexes $(CO)_nTM–ER$ and $TM(ER)_n$ with Group 13 ligand atoms B–Tl may be summarized as follows.

1. The bond dissociation energies of the TM–ER bonds are rather high, showing for the elements E the trend B > Al > Ga ~ In > Tl. The trend is the same for transition metals of Groups 6, 8 and 10 with different R substituents which may or may not be strong π donors.
2. The TM–ER bonds investigated so far have a large ionic character besides the covalent contributions which come from the RE → TM σ-donation and RE ← TM π-backdonation.
3. The ligands ER which have strong π-donor groups R with lone-pair electrons (F, NR_2, O^-, Cl) or with π-electrons (Cp) may still have significant RE ← TM π-backdonation particularly if R is an electronegative substituent.
4. Transition metal–ligand bonds TM–ER where R is not a strong π-donor exhibit enhanced RE ← TM π-backdonation.
5. The TM–ER bond dissociation energy depends on the contributions of the orbital interactions ΔE_σ and ΔE_π, but also on the contributions of the Pauli repulsion (ΔE_{Pauli}), charge interactions (ΔE_{elst}) and fragment preparation energies (ΔE_{prep}).

5. Conclusion and outlook

The coordination chemistry of Group 13 diyl complexes has blossomed in the last few years, and it can be expected that further progress will be made in the near future. An exciting aspect of the field is the cooperation and mutual challenge of theorist and experimentalists in breaking new ground. There are still only a few transition metal elements for which stable compounds with terminal TM–ER bonds are known. Accurate calculations may help to design experiments aiming at the synthesis of further promising candidates. One aspect which has not been studied so far concerns compounds with TM=ER bonds where the transition metal is in a high oxidation state and E has the formal oxidation state +3, which relates these compounds to Schrock-type alkylidenes [25d]. Theoretical studies are needed to find out if Group 13 'diylidenes' might become isolable. Calculations do not replace experiments, but they are helpful to guide synthetic attempts towards more fruitful avenues.

An area where only theory can give a satisfactory answer is the question of the nature of the TM–ER bond. It has become customary to correlate experimental results with ad hoc bonding models with the goal to bring an ordering scheme into the trends that are found in inorganic chemistry [34]. A popular example is the correlation between CO stretching frequencies in TM complexes and the alleged π-acceptor ability of a ligand *trans* to CO. While this is a helpful heuristic devise to order ligands into a scale, it does not prove anything about the factors which actually influence the C–O stretching mode, and it does not give insight into the nature of the TM–ligand bond. The latter can only be given by a careful analysis of accurate quantum chemical calculations.

Acknowledgements

This work was supported by the Deutsche Forschungsgemeinschaft and the Fonds der Chemischen Industrie. Excellent service by the Hochschulrechenzentrum of the Philipps-Universität Marburg is gratefully acknowledged. Additional computer time was provided by the HLRZ Stuttgart and the HHLRZ Darmstadt.

References

[1] R.A. Fischer, J. Weiß, Angew. Chem. 111 (1999) 3002; Angew. Chem. Int. Ed. Engl. 38 (1999) 2830.
[2] J. Weiß, D. Stetzkamp, B. Nuber, R.A. Fischer, C. Boehme, G. Frenking, Angew. Chem. 109 (1997) 95; Angew. Chem. Int. Ed. Engl. 36 (1997) 70.
[3] A.H. Cowley, V. Lomeli, A. Voigt, J. Am. Chem. Soc. 120 (1998) 6401.
[4] H. Braunschweig, C. Kollann, U. Englert, Angew. Chem. 110 (1998) 3355; Angew. Chem. Int. Ed. Engl. 37 (1998) 3179.
[5] J. Su, X.-W. Li, R.C. Crittendon, C.F. Campana, G.H. Robinson, Organometallics 16 (1997) 4511.
[6] W. Uhl, M. Pohlmann, R. Wartchow, Angew. Chem. 110 (1998) 1007; Angew. Chem. Int. Ed. Engl. 37 (1998) 961.
[7] W. Uhl, M. Benter, S. Melle, W. Saak, G. Frenking, J. Uddin, Organometallics 18 (1999) 3778.
[8] H. Werner, Angew. Chem. 102 (1990) 1109; Angew. Chem. Int. Ed. Engl. 29 (1990) 1077.
[9] F.M. Bickelhaupt, F.M., Radius, A.W. Ehlers, R. Hoffmann, E.J. Baerends, New J. Chem. (1998) 1.
[10] U. Radius, F.M. Bickelhaupt, A.W. Ehlers, N. Goldberg, R. Hoffmann, Inorg. Chem. 37 (1998) 1080.
[11] A.W. Ehlers, E.J. Baerends, F.M. Bickelhaupt, U. Radius, Chem. Eur. J. 4 (1998) 210.
[12] (a) R. Dagani, Chem. Eng. News 76 (11) (1998) 31. (b) R. Dagani, Chem. Eng. News 75 (24) (1997) 9.
[13] F.A. Cotton, X. Feng, Organometallics 17 (1998) 128.
[14] C. Boehme, G. Frenking, Chem. Eur. J. 5 (1999) 2184.
[15] R.A. Fischer, M.M. Schulte, J. Weiss, L. Zsolnai, A. Jacobi, G. Huttner, G. Frenking, C. Boehme, S.F. Vyboishchikov, J. Am. Chem. Soc. 120 (1998) 1237.
[16] J. Uddin, C. Boehme, G. Frenking, J. Am. Chem. Soc., submitted for publication.
[17] C. Boehme, C. Doctoral thesis, Philipps-Universität, Marburg, 1998.
[18] (a) P.J. Hay, W.R. Wadt, J. Chem. Phys. 82 (1985) 299. (b) L.F. Pacios, P.A. Christiansen, J. Chem. Phys. 82 (1985) 2664. (c) M.M. Hurley, L.F. Pacios, P.A. Christiansen, R.B. Ross, W.C. Ermler, J. Chem. Phys. 84 (1986) 6840. (d) L.A. LaJohn, P.A. Christiansen, R.B. Ross, T. Atashroo, W.C. Ermler, J. Chem. Phys. 87 (1987) 2812. (e) R.B. Ross, J.M. Powers, T. Atashroo, W.E.C. Ermler, L.A. LaJohn, P.A. Christiansen, J. Chem. Phys. 93 (1990) 6654. (f) W.J. Stevens, M. Krauss, H. Basch, P.G. Jasien,Can. J. Chem. 70 (1992) 612. (g) M. Dolg, U. Wedig, H. Stoll, H.J. Preuss, Chem. Phys. 86 (1987) 866. (h) D. Andrae, U. Häußermann, M. Dolg, H. Stoll, H. Preuss, Theor. Chim. Acta 77 (1990) 123.
[19] (a) G. Frenking, I. Antes, M. Boehme, S. Dapprich, A.W. Ehlers, V. Jonas, A. Neuhaus, M. Otto, R. Stegmann, A. Veldkamp, S.F. Vyboishchikov, in: K.B. Lipkowitz, D.B. Boyd (Eds.), Reviews in Computational Chemistry, vol. 8, VCH, New York, p. 63–144, 1996. (b) T.R. Cundari, M.T. Benson, M.L. Lutz, S.O. Sommerer, in: K.B. Lipkowitz, D.B. Boyd (Eds.), Reviews in Computational Chemistry, vol. 8, VCH, New York, p. 145–202, 1996. (c) T. Ziegler, Chem. Rev. 91 (1991) 651.
[20] T. Ziegler, A. Rauk, Theor. Chim. Acta 46 (1977) 1.
[21] K. Morokuma, Acc. Chem. Res. 10 (1977) 294.
[22] F.M. Bickelhaupt, E.J. Baerends, Rev. Comput. Chem., in print.

[23] S. Dapprich, G. Frenking, J. Phys. Chem. 99 (1995) 9352.
[24] (a) M.J.S. Dewar, Bull. Soc. Chim. Fr. 18 (1951) C79. (b) J. Chatt, L.A. Duncanson, J. Chem. Soc. (1953) 2929.
[25] (a) G. Frenking, U.J. Pidun, Chem. Soc. Dalton Trans. (1997) 1653. (b) U. Pidun, G. Frenking, J. Organomet. Chem. 525 (1996) 269. (c) U. Pidun, G. Frenking, Organometallics 14 (1995) 5325. (d) S.F. Vyboishchikov, G. Frenking, Chem. Eur. J. 4 (1998) 1428. (e) S.F. Vyboishchikov, G. Frenking, Chem. Eur. J. 4 (1998) 1439.
[26] (a) E.R. Davidson, K.L. Kunze, F.B.C. Machado, S.J. Chakravorty, Acc. Chem. Res. 26 (1993) 628. (b) K.L. Kunze, E.R. Davidson, J. Phys. Chem. 96 (1992) 2129. (c) F.B.C. Machado, E.R. Davidson, J. Phys. Chem. 97 (1993) 4397.
[27] A. Diefenbach, F.M. Bickelhaupt, G. Frenking, J. Am. Chem. Soc., submitted for publication.
[28] (a) S.H. Strauss, Chemtracts Inorg. Chem. 10 (1997) 77. (b) A.J. Lupinetti, G. Frenking, S.H. Strauss, Angew. Chem. 110 (1998) 2229; Angew. Chem. Int. Ed. Engl. 37 (1998) 2113.
[29] (a) A.J. Lupinetti, S. Fau, G. Frenking, S.H. Strauss, J. Phys. Chem. A 101 (1997) 9551. (b) A.S. Goldman, K.J. Krogh-Jespersen, Am. Chem. Soc. 118 (1996) 12159.
[30] (a) K.L. D'Amico, M. Trenary, N.D. Shinn, E.I. Solomon, F.R. McFeely, J. Am. Chem. Soc. 104 (1982) 5102. (b) D. Tevault, K. Nakamoto, Inorg. Chem. 15 (1976) 1282. (c) R.L. DeKock, A.C. Sarapu, R.F. Fenske, Inorg. Chem. 10 (1971) 38. (d) J.B. Johnson, W.G. Klemperer, J. Am. Chem. Soc. 99 (1977) 7132. (e) T.A. Albright, J.K. Burdett, M.H. Whangbo, Orbital Interactions in Chemistry, Wiley, New York, 1985, p. 82. (f) Ch. Elschenbroich, A. Salzer, Organometallics, second ed., VCH, Weinheim, 1992, p. 227.
[31] G.J. Irvine, M.J.G. Lesley, T.B Marder, N.C. Norman, C.R. Rice, E.G. Robins, W.R. Roper, G.R. Whittell, L.J. Wright, Chem. Rev. 98 (1998) 2685.
[32] P. Jutzi, B. Neumann, G. Reumann, H.G. Stammler, Organometallics 17 (1998) 1305.
[33] G. Schmid, W. Petz, H. Nöth, Inorg. Chim. Acta 4 (1970) 423.
[34] D.M.P. Mingos, Essential Trends in Inorganic Chemistry, Oxford University Press, Oxford, 1998.
[35] A.W. Ehlers, G. Frenking, Organometallics 14 (1995) 423.